First observation of high-spin states in ^{214}Po: Probing the valence space beyond ^{208}Pb

A. Astier, M.-G. Porquet

First observation of high-spin states in ^{214}Po: Probing the valence space above ^{208}Pb

Alain Astier[1] and Marie-Geneviève Porquet[1]
[1] *CSNSM, IN2P3/CNRS and Université Paris-Sud, F-91405 Orsay Campus, France*
(Dated: December 21, 2010)

Excited states in ^{214}Po have been populated using the ^{18}O + ^{208}Pb reaction at 85 MeV beam energy and studied with the Euroball IV γ-multidetector array. The level scheme has been built up to $\sim$ 2.7 MeV excitation energy and spin $I = 12\ \hbar$ from the triple γ coincidence data. Spin and parity values of most of the observed states have been assigned from the γ-angular properties. The configurations of the yrast states are discussed using results of empirical shell-model calculations and by analogy with the neighbouring nuclei. The ^{214}Po level scheme established in this work constitutes an important step for the determination of the effective nucleon-nucleon interactions beyond $N = 126$.

PACS numbers: 25.70.Hi, 27.80.+w, 23.20.-g, 21.60.Gx

I. INTRODUCTION

The knowledge of the excited levels of nuclei lying north-east of ^{208}Pb remains fragmentary since most of these nuclei with $Z > 82$ and $N > 126$ cannot be populated *via* the standard reactions because of the lack of suitable stable projectile-target combinations. In many cases, one can only rely on decay studies (α and/or β) which unfortunately give access to a very restricted range of spin values. Such a situation prevents us to follow the behaviours along whole isotopic or isotonic series, while it is so fruitful for the identification of the involved configurations. This is for instance the case for the study of the filling of the $\nu g_{9/2}$ orbital which is expected to play the major role in $^{211-220}$Po. Whereas the high-spin states of ^{210,212}Po isotopes could be investigated by fusion-evaporation reactions [1] and the states up to 8^+ of ^{216,218}Po by the β-decay of Bi isotopes [2, 3], there was, up to now, no candidate for the medium-spin states of ^{214}Po. Because of the low spin of the parent ^{214}Bi ($I^\pi = 1^-$), the spin values of the observed states in ^{214}Po are mainly 0, 1 or 2 [1]. The synthesis of this nucleus, with 2 protons and 4 neutrons above the heaviest stable nucleus, is not an easy task since such a transfer of 6 nucleons is a very peculiar exit channel of reactions induced by heavy ions, having likely a very low cross section.

We have performed a very detailed identification of all the nuclides produced in the ^{18}O+^{208}Pb reaction at 85 MeV thanks to their gamma decays, the great sensitivity and high efficiency of the Euroball IV germanium array being decisive for that purpose. In addition to the $\sim$150 fission fragments, which were the main objective of the experiment [4], as well as the $^{222-224}$Th isotopes corresponding to the expected fusion-evaporation reaction, we have found γ-ray cascades emitted by several trans-lead nuclei produced by various transfer reactions.

Our results on ^{212}Po have been recently published [5, 6]. In the present paper, we report on high-spin excited states in ^{214}Po, which are identified for the first time. In addition to the usual analysis of the high-fold coincidences to build the level scheme, the angular distributions and anisotropy ratios of γ-rays have been measured to assign the spin values. Moreover the existence of isomeric states has been looked for from the Ge detector timing information. The yrast states of ^{214}Po which have been obtained up to $I^\pi = 12^+$ are discussed using an empirical shell-model approach.

II. EXPERIMENTAL METHODS AND DATA ANALYSIS

We have used the ^{18}O+^{208}Pb reaction, the ^{18}O beam with an energy of 85 MeV being provided by the Vivitron tandem of IReS (Strasbourg). A 100 mg/cm^2 self-supporting target of ^{208}Pb was employed, which was thick enough to stop the recoiling nuclei. It is worth noting that due to this large thickness, the ^{18}O beam was stopped in the Pb target too, and therefore the incident energy covered a large range of values, above and below the Coulomb barrier. The de-exciting γ-rays were recorded with the EUROBALL IV array consisting of 71 Compton-suppressed Ge detectors [7] (15 cluster germanium detectors placed in the backward hemisphere with respect to the beam, 26 clover germanium detectors located around 90°, 30 tapered single-crystal germanium detectors located at forward angles). Each cluster detector is composed of seven closely packed large-volume Ge crystals [8] and each clover detector consists of four smaller Ge crystals [9]. The 239 Ge crystals of the Euroball array could be grouped into 13 rings, with the following angles with respect to the beam axis, 15.5° (5 crystals), 34.6° (10), 52.3° (15), 72.2° (26), 80.9° (26), 99.1° (26), 107.5° (26), 122.6° (10), 130.5° (30), 138.7° (25), 148.1° (15), 155.9° (15), and 163.5° (10), i.e. 3 rings forward, 4 rings close to 90° and 6 rings backward with respect to the beam axis.

Events were recorded on tape when at least 3 unsuppressed Ge detectors fired in prompt coincidence. In this way, a set of $\sim 4 \times 10^9$ three- and higher-fold events were available for subsequent analysis, but only a small part of these data corresponds to ^{214}Po events. Indeed the main objective of the experiment was actually the study of the fusion-fission channel which leads to the production of

the high-spin states of ~ 150 fragments, mainly located on the neutron-rich side of the valley of stability [4]. The ^{214}Po study became itself a goal when it turned out that its main γ lines were strong enough in our data set to be identified and precisely analyzed. The production of ^{214}Po in the ^{18}O+^{208}Pb reaction comes from a channel which likely involves two steps, the breakup of the ^{18}O projectile and the fusion of the light partner and the target. From our data set, we have estimated that the cross section of this channel is 0.5-1 mb.

Various procedures have been used for the offline analysis in order to fully characterize the excited levels of ^{214}Po (excitation energy, spin and parity values). Both multi-gated spectra and three-dimensional 'cubes' have been built and analyzed with the Radware package [10], starting from the first transition deexciting the 2^+ state [1] in order to identify the new transitions and to build the level scheme.

The angular distributions of the γ-rays with respect to the beam axis have been analyzed to determine their multipole orders. In order to characterize the transitions having too weak intensity to be analyzed in that way, their anisotropies have been determined using the intensities measured at two angles relative to the beam axis, R_{ADO}=$I_\gamma(39.3°)$/ $I_\gamma(76.6°)$, these two angles being the average angle of the tapered and cluster detectors in the one hand, and the average angle of the clover detectors in the other hand, when taking into account the symmetry of the distribution around 90°.

The timing information from the germanium detectors have been used to measure the half-life of the 8^+ yrast state. The procedures were checked using the delayed coincidences of isomeric states of various nuclei produced in this experiment, as described in ref. [11].

III. EXPERIMENTAL RESULTS

The study of the β^- decay of ^{214}Bi goes back to the early days of nuclear physics. This remained the sole source of information for ^{214}Po, since their excited levels have not reached by any nuclear reaction to date [1]. Because of the low spin of the parent ^{214}Bi ($I^\pi = 1^-$), the spin values of the observed states are mainly 0, 1 or 2. The second excited state at 1015 keV was assigned a most probable I^π of 4^+ from the directional correlation coefficients for the 406-609 keV cascade [12], while the gamma intensity imbalance found for this level led to $\log ft = 9.6 \pm 0.1$, which is strongly at variance with the value expected for a third forbidden transition ($\log ft \sim 18$).

In order to identify the unkown transitions depopulating the yrast states of ^{214}Po, we have first looked into spectra gated by the $K_{\alpha 1}$ X-rays[1] of Po. The spectrum of γ-rays in coincidence with *two* $K_{\alpha 1}$ X-rays of Po displays, in addition to the strong transitions emitted by ^{212}Po [5, 6], the $2^+ \rightarrow 0^+$ transition of ^{214}Po (609 keV). We have then analyzed the spectrum in double coincidence with this transition and the $K_{\alpha 1}$ X-ray of Po (see Fig. 1(a)). Three transitions of 244, 324, and 405 keV are

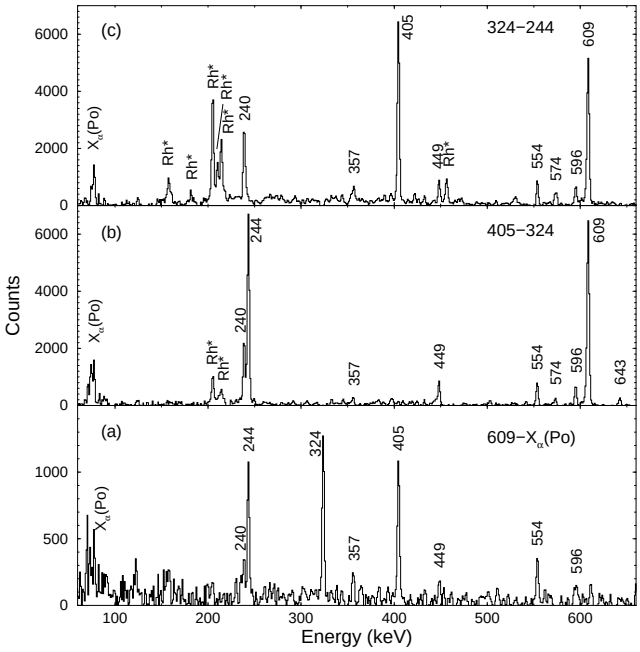

FIG. 1: Spectra of γ-rays in double coincidence with (a) the first transition of ^{214}Po (609 keV) and the $K_{\alpha 1}$ X-ray of Po, (b) the 405 keV and 324 keV transitions, and (c) the 324 keV and 244 keV transitions. The lines, marked with a star, are contaminants due to several Rh isotopes (see text).

clearly observed and assigned to ^{214}Po. We have then analyzed all the spectra in double coincidence with them (see, as examples, the spectra displayed in Figs. 1(b) and 1(c)), as well as many spectra in triple coincidence with the newly identified γ-rays. It is worth noting that some of the double-gated spectra display contaminants, as ~ 150 nuclei are produced at high spin in the fusion-fission reaction ^{18}O+^{208}Pb [4], that gives several thousands of γ-lines close in energy. In particular, two strong transitions of ^{109}Rh (324 and 242 keV) produce many contaminant lines in the spectrum of Fig. 1(c): They are emitted either by ^{109}Rh or by its complementary fragments, $^{110-111-112}$Rh (see refs. [13, 14]).

The level scheme built from all the analysed coincidence relationships is shown in Fig. 2. A 671 keV line is

[1] Low-energy transitions, such as the X-rays of Po, are clearly observed in our work since we used a very low threshold for triggering the CFD discriminator of each Ge channel. This was allowed by the VXI electronic cards of the Euroball array. For that purpose, the lower thresholds of the 239 channels were carefully checked at the beginning of the data acquisition.

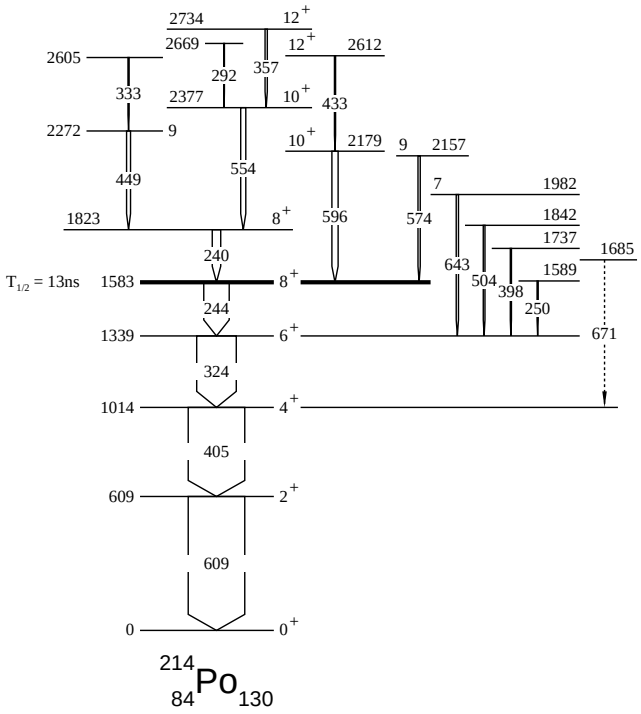

FIG. 2: Level scheme of ^{214}Po determined in this work. The half-life of the 8^+_1 state is 13(1) ns (see text). The width of the arrows is representative of the intensity of the γ-rays.

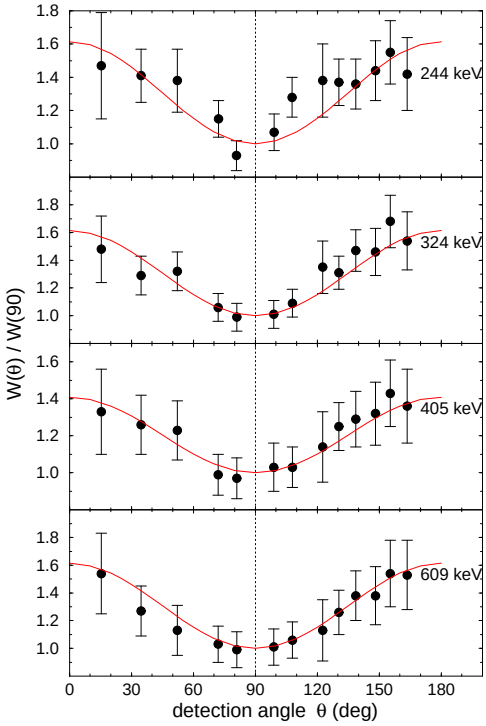

FIG. 3: (color online) Angular distribution of the most intense transitions of ^{214}Po produced in the ^{18}O + ^{208}Pb reaction. Solid (red) lines are the fits using the standard Legendre polynomials (results are given in Table I).

clearly seen in the spectrum gated by the two first yrast transitions (609 keV and 405 keV). Nevertheless, in the absence of any other confirmation of its origin, it is not firmly attributed to ^{214}Po.

In order to determine the spin values of the ^{214}Po states, we have firstly analyzed the angular distributions of the four most intense transitions. The results, displayed in Fig. 3, indicate that the 405, 324 and 244 keV transitions are quadrupole transitions with $\Delta I = 2$, such as the 609 keV one ($2^+ \rightarrow 0^+$), already known. Thus the yrast cascade of ^{214}Po is newly identified up to spin 8^+, at 1583 keV. The location of the 4^+ state at 1014 keV is then fully confirmed, in agreement with the suggestion of ref. [12], the feature of the logft value mentioned above likely comes from the incompleteness of the β-decay scheme of ^{214}Bi. It is worth recalling that the intensity imbalance of the 1015-keV 4^+ state was only 0.094(19) per 100 β-decays [1].

We have gathered in Table II all the properties of the transitions assigned to ^{214}Po from this work. In particular, the third column gives the R$_{ADO}$ values which allow us to determine the spin values of most of the states lying above 1.6 MeV.

The 240 keV transition is located jut above the 8^+ yrast state (see Fig. 2). Without any experimental result on its multipole order at hand, we could assume that it is the next $\Delta I = 2$ transition, leading to the 10^+_1 state at 1823 keV. The actual result is more complex, as the

TABLE I: Angular distribution coefficient (a$_2$) and multipole order of the most intense γ-rays of ^{214}Po.

E$_\gamma$	a$_2$ [a]	multipole order	spin sequence
609.0	+0.34(5)	ΔI=2 quadrupole	$2^+ \rightarrow 0^+$
405.4	+0.25(5)	ΔI=2 quadrupole	$4^+ \rightarrow 2^+$
324.4	+0.3(1)	ΔI=2 quadrupole	$6^+ \rightarrow 4^+$
244.1	+0.30(15)	ΔI=2 quadrupole	$8^+ \rightarrow 6^+$

[a]The number in parenthesis is the error in the last digit.

R$_{ADO}$ value of the 240 keV transition is slightly less than 1.0 (see Table II) and not around 1.3, the value of the $\Delta I = 2$ transitions, such as the 244 keV transition which depopulates the 8^+ yrast state. The contrasting behaviour of the 240 keV and 244 keV transitions is clearly demonstrated in Fig. 4, the intensity ratio of these two transitions is not the same in the two spectra registered at different detection angles, $\theta_{mean} = 39.3°$ (tapered and cluster detectors) and $\theta_{mean} = 76.6°$ (clover detectors) respectively. A weak anisotropy, such as that displayed by the 240 keV transition, is foreseen when a transition is of mixed multipole type (dipole + quadrupole), for particular values of the mixing ratio, the transition being either stretched, $\Delta I = 1$, or non-stretched, $\Delta I = 0$.

To go further, we have extracted the internal conversion electron coefficients of some transitions of ^{214}Po by

TABLE II: γ-ray transition energies (E_γ), relative γ intensities (I_γ), angular distribution ratios (R_{ADO}), and level and spin assignments for the ^{214}Po nucleus.

E_γ [a] (keV)	I_γ [b] [c]	R_{ADO}	E_i (keV)	E_f (keV)	I_i^π	I_f^π
239.6	15(2)	0.95(5)	1822.5	1582.9	8^+	8^+
244.1	44(5)	1.31(7)	1582.9	1338.8	8^+	6^+
250.2	2.0(8)		1589.0	1338.8		6^+
292.4	1.2(6)		2669.3	2376.9		10^+
324.4	70(5)	1.30(8)	1338.8	1014.4	6^+	4^+
333.0	2.0(8)		2604.5	2271.5		9
356.8	4(1)	1.3(3)	2733.8	2376.9	12^+	10^+
398.0	1.8(6)		1736.8	1338.8		
405.4	100	1.26(8)	1014.4	609.0	4^+	2^+
433.2	2.5(10)	1.2(2)	2611.9	2178.7	12^+	10^+
449.0	7.4(12)	0.76(11)	2271.5	1822.5	9	8^+
503.5	3(1)		1842.3	1338.8		
554.5	8.5(13)	1.34(17)	2376.9	1822.5	10^+	8^+
574.4	3.8(11)	0.8(2)	2157.3	1582.9	9	8^+
595.8	11(1)	1.32(15)	2178.7	1582.9	10^+	8^+
609.0	-	1.24(8)	609.0	0.0	2^+	0^+
642.9	3.7(11)	0.6(2)	1981.7	1338.8	7	6^+
670.5	3.8(12)		1684.9	1014.4		4^+

[a] Uncertainties in transition energies are typically between 0.1 and 0.5 keV.

[b] Intensities measured in this experiment (i.e. with the requirement that a minimum of three unsuppressed Ge detectors fired in prompt coincidence) are normalized to the value of the transition populating the 2_1^+ state, I_γ(405.4 keV) = 100.

[c] The number in parenthesis is the error in the last digit.

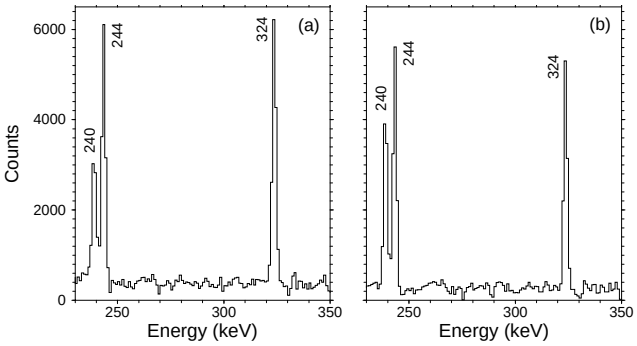

FIG. 4: Low energy part of the γ-ray spectra showing the yrast transitions of ^{214}Po detected at a mean angle of 39.3° by the tapered and cluster detectors (a) and at a mean angle of 76.6° by the clover detectors (b).

analyzing the relative intensities of transitions in cascade. The intensity imbalances of the 244 keV and the 240 keV γ-rays measured in spectra in double coincidence with at least one transition located above them in the level scheme lead to α_{tot}(244 keV)=0.25(5) and α_{tot}(240 keV)=0.7(1). While the first value is in good agreement with the theoretical value for E2 multipolarity [15], the second one implies that the 240 keV transition is strongly mixed, 65(15)% M1 + 35(15)% E2.

Using the theoretical coefficients of angular distribution of gamma rays from aligned nuclei [16], we have computed the parameters of such a strongly mixed transition assuming either $\Delta I = 1$ or $\Delta I = 0$, and taking into account the two possible signs of the mixing ratio. A weak anisotropy is obtained when the transition is non-stretched, with a negative mixing ratio. Thus the spin value of the 1823 keV level is unambiguously assigned, $I^\pi = 8^+$.

Noteworthy is the fact that the large value of the internal conversion electron coefficient of the 240 keV transition is confirmed by the loss in intensity of its γ line in the spectra when gated by the X-rays of Po. A first example is given in Fig. 1, the intensity of the 240 keV line is weaker in Fig. 1(a) than in Fig. 1(b), as compared to the intensity of the 244 keV line. A second example is shown in Fig. 5, the 240 keV line is stronger than the 357 keV one in the spectrum gated by the 554 keV and the 405 keV transitions (see Fig. 5(a)), while it has almost vanished in the spectrum gated by the 554 keV transition and the $K_{\alpha 1}$ X-ray of Po (see Fig. 5(b)). Such

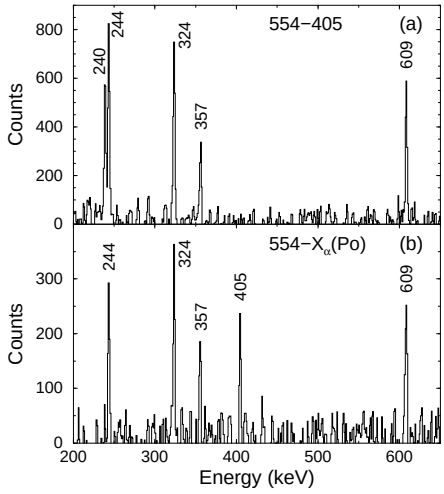

FIG. 5: Spectra of γ-rays in double coincidence with (a) the 554 keV and 405 keV transitions, (b) the 554 keV transition and the $K_{\alpha 1}$ X-ray of Po.

a behaviour corroborates the method of γ-ray identification by means of the $K_{\alpha 1}$ X-ray of Po, used in the present work.

The spin and parity values of the levels lying above the 1583 keV and 1823 keV states have been chosen according to the R_{ADO} values of the involved γ-rays (see Table II). Aside from a few levels with odd spin values, the yrast structure comprises two states with $I^\pi = 10^+$ and two states with $I^\pi = 12^+$.

The timing information from the germanium detectors have been used to look for isomeric states in the 10-300 ns range. The time distributions between the γ-ray emissions of all the yrast states have been systematically analyzed. Typical spectra are shown in Fig. 6, they are

compared with the case of prompt coincidences (curve filled in gray) measured for the 4^+ yrast state of ^{212}Po, obtained in the same work [5, 6].

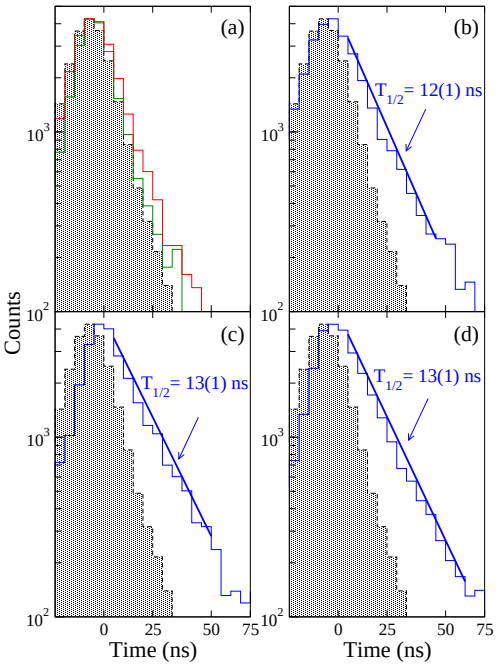

FIG. 6: (color online) Time distributions between the emissions of γ-rays of ^{214}Po showing either prompt coincidences -curves in red and green, panel (a)- or delayed ones corresponding to the decay of the 1583 keV state -curves in blue, panels (b), (c), and (d)-, they are compared with an example of γ-rays of ^{212}Po in prompt coincidences, shown with the curve filled in gray (see text).

In Fig. 6(a), the green spectrum is the time distribution between the emission of the 324 keV γ-ray and that of either the 405 keV or the 609 keV γ-rays, while the red spectrum is the time distribution between the emission of the 244 keV γ-ray and that of either the 324 keV or the 405 keV or the 609 keV γ-rays. They show that the decays of the 4^+ and 6^+ states are prompt. In Fig. 6(b), Fig. 6(c), and Fig. 6(d), the blue spectra are the time distributions between the emission of the 240 keV, 554 keV, and 449 keV transitions, respectively, and that of one transition located below the 1583 keV state. They establish that the half-life of the 8_1^+ state is 13(1) ns. Then the value of the B(E2) reduced transition probability of the 244 keV transition is 41(3) e^2fm^2, i.e. 0.54(4) *W.u.*, taking into account the theoretical value of its internal conversion coefficient (α_{tot}(E2)=0.24). This result will be discussed in the next section.

It is noteworthy that none of the γ-ray of ^{214}Po measured in the present work exhibits Doppler shift or broadening, meaning that none of the observed states have lifetimes shorter than 1 ps. This is at variance with the ^{212}Po results obtained in the same experiment [5, 6]. Nevertheless it cannot be excluded that states decaying by very enhanced E1 transitions also occur in ^{214}Po, but being much less populated than the yrast states, their identification would need much more statistics than that obtained in the present work.

IV. DISCUSSION

With two protons and four neutrons more than the doubly-magic ^{208}Pb, ^{214}Po would display a low-lying structure coming from the excitations of a few single-particle states in the mean field of the core, i.e. $\pi h_{9/2}$ and $\pi f_{7/2}$ on the one hand, $\nu g_{9/2}$ and $\nu i_{11/2}$ on the other hand. Using the experimental results of the neighbouring nuclei and assuming that the various configurations do not mix, we easily get the energies of some unperturbed states in ^{214}Po, as shown in Fig. 7 using different symbols:

- Eigtheen states are expected from the $(\nu g_{9/2})^4$ configuration: One seniority-0 state (0^+), four seniority-1 states (2^+, 4^+, 6^+, 8^+) and thirteen seniority-2 states (up to 12^+). Their relative energies are computed using the energies of the $(\nu g_{9/2})^2$ multiplet (known in ^{210}Pb [1]) and the coefficients of fractional parentage (CFP), assuming that the shell-model Hamiltonian contains at most two-body interactions (see for instance ref. [17]). The energies of the *yrast* states are drawn with the red full circles (among the seniority-2 states, we have only reported those with the highest spin values, 8^+, 9^+, 10^+, and 12^+).

- The two-neutron configuration, $(\nu g_{9/2})^1(\nu i_{11/2})^1$, gives rise to a multiplet with $I^\pi = 1^+$ to 10^+. The 8^+ and 10^+ states are known in ^{210}Pb (see the stars in magenta).

- The energies of the 2^+, 4^+, 6^+, and 8^+ states from the two-proton configuration $(\pi h_{9/2})^2$ come from ^{210}Po [1] (see the blue filled diamonds).

- The two-proton configuration, $(\pi h_{9/2})^1(\pi f_{7/2})^1$, gives rise to a multiplet with $I^\pi = 1^+$ to 8^+. The 8^+ state is known in ^{210}Po (see the violet filled square).

Then we compare the experimentally observed states of ^{214}Po (Fig. 2) to the results given in Fig. 7. As for the yrast states up to 8^+, the involved configurations are certainly more complex than $(\nu g_{9/2})^4$, since the measured 4^+, 6^+, and 8^+ states are not so close in energy. It is worth recalling that the first yrast states of ^{212}Pb have been identified [1] and the level spectrum (see the right part of Fig. 7) is in good agreement with the prediction of the $(\nu g_{9/2})^4$ configuration.

Since at least four 8^+ states are expected close in energy in ^{214}Po, this could explain why two 8^+ states are populated in the yrast decay studied in the present

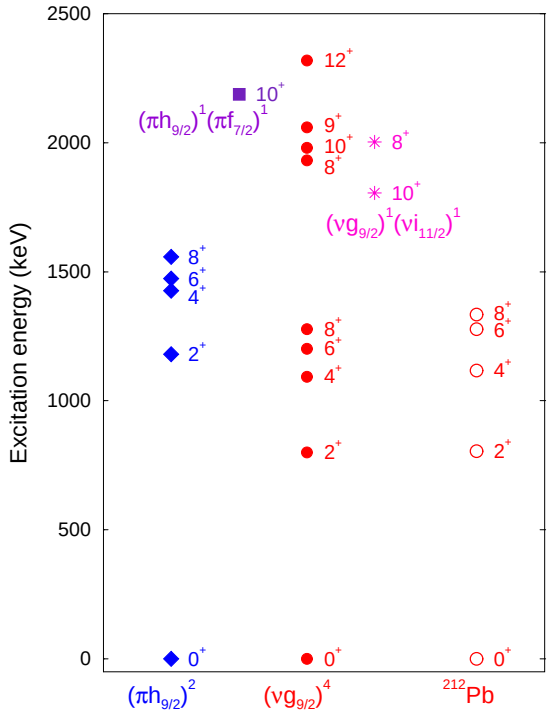

FIG. 7: (color online) Energies for expected states in ^{214}Po, (i) from the $(\nu g_{9/2})^4$ configuration calculated using empirical shell model (red full circles), (ii) from the $(\nu g_{9/2})^1(\nu i_{11/2})^1$ configuration measured in ^{210}Pb (stars in magenta), (iii) from the $(\pi h_{9/2})^2$ configuration measured in ^{210}Po (blue filled diamonds), (iv) from the $(\pi h_{9/2})^1(\pi f_{7/2})^1$ configuration measured in ^{210}Po (violet filled square). The experimental states of ^{212}Pb are shown for comparison (red empty circles).

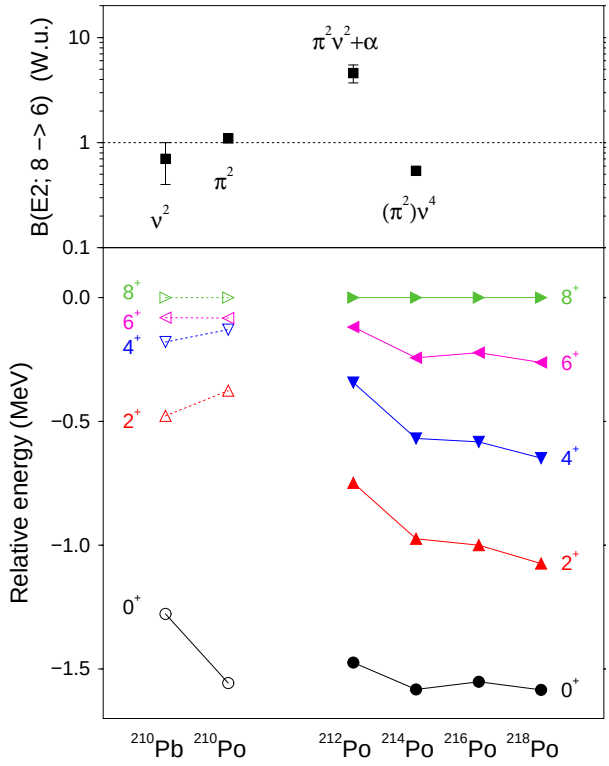

FIG. 8: (color online) **Bottom**: Evolution of the first energy levels in the even Po isotopes, $^{210-218}$Po, and in ^{210}Pb. The energies of the 8_1^+ states are adjusted to a constant value (see text). **Top**: Experimental values of the reduced transition probabilities B(E2; $8^+ \rightarrow 6^+$) for ^{210}Pb, ^{210}Po, and ^{212,214}Po. Data are taken from refs. [1–3, 5, 6] and this work.

work. As for the higher spin states, the breaking of two-nucleon pairs being not fully considered in the computation leading to Fig. 7, several other 10^+ and 12^+ states are foreseen, such as from the $(\nu g_{9/2})^3(\nu i_{11/2})^1$ and $(\nu g_{9/2})^2(\pi h_{9/2})^2$ configurations.

In summary, the structure of the high spin states of ^{214}Po identified in this work likely involve the breaking of one and two pairs of nucleons in the four orbits above the magic gaps, $\pi h_{9/2}$ and $\pi f_{7/2}$, $\nu g_{9/2}$ and $\nu i_{11/2}$. It would be instructive to compare our experimental results to shell-model (SM) calculations using realistic effective interactions. This is discussed below.

In this second part of the discussion, we compare the first excited states of ^{214}Po to the ones of the neighbouring isotopes. Fortunately the spin value of the β-decaying state of ^{216,218}Bi is high, $> 6\hbar$ [1] (the one of ^{214}Bi is 1^-, as said above). The study of these decays [2, 3] gave the first results on the medium-spin states of ^{216,218}Po, with I^π up to 8^+. The evolution of these levels in the $^{210-218}$Po isotopes and in ^{210}Pb is shown in the bottom part of Fig. 8, the energies of the 8_1^+ states being adjusted to a constant value in order to enhance the typical pattern of states due to a two-nucleon configuration, if any. The yrast states of the three isotopes ^{214,216,218}Po have quasi-constant relative energies, showing that their configurations do bear strong resemblance. According to the SM calculations based on the Kuo-Herling interaction, performed in ref. [3], the sequence of the 4_1^+, 6_1^+, and 8_1^+ states of ^{218}Po should be very compressed (as those of ^{210}Po), at variance with the experimental results. This calls for a review of the realistic effective interactions to improve the predictions in this mass region.

The first levels of ^{212}Po do not follow the trend of the heavier isotopes, even though the distance in energy between the 0^+ and the 8^+ states is almost the same. It is worth recalling that '$\alpha+$ ^{208}Pb' cluster structures have been recently found in ^{212}Po, which coexist (and eventually mix) with single-particle excitations [6]. Such mixings are likely responsible of the large variation of the level energies shown in the bottom part of Fig. 8.

To go further and to have a deeper insight into the wave functions of the yrast states of heavy Po isotopes, we use the values of the reduced transition probabilities, particularly these of B(E2; $8_1^+ \rightarrow 6_1^+$) which have been measured in four cases (see the top part of Fig. 8). As expected, the value of ^{210}Po is above that of ^{210}Pb, owing to their different excitation processes, π^2 *versus* ν^2. The large value

measured in ^{212}Po can be explained by the 'α+ ^{208}Pb' cluster content of the wave functions [6]. As regards ^{214}Pb, it is worth pointing out that the B(E2; $8^+ \rightarrow 6^+$) value measured in the present work (0.54(4) *W.u.*) is of the same order of magnitude than the one of ^{210}Pb, with the ν^2 configuration. Thus a one-neutron-pair breaking is likely the main excitation process of the 8_1^+ state in the heavy Po isotopes. Such an assumption could be checked by measuring the half-life of the 8_1^+ state of ^{216,218}Po. Taking into account the energies of the E2 decaying transition (223 keV and 263 keV, respectively) and their conversion coefficient, and assuming B(E2; $8^+ \rightarrow 6^+$)= 0.5 *W.u.*, we expect $T_{1/2}(8_1^+) = 20$ ns and 10 ns respectively. At least, the measurement of the first one could be easily performed using the timing information from germanium detectors.

V. SUMMARY AND CONCLUSIONS

High spin states of ^{214}Po up to 12^+ have been identified for the first time. This neutron-rich isotope has been produced in the ^{18}O+^{208}Pb reaction, the γ-rays being detected using the Euroball IV γ-multidetector array. Spin and parity values of most of the observed states have been assigned from the γ-angular distributions and DCO ratios. An isomeric state which decays by an E2 transition has been established at spin 8^+. The configurations of the yrast states have been discussed using results of empirical shell-model calculations. Moreover, the first four excited states measured in ^{214}Po have been found very similar to those known in ^{216,218}Po , showing that it does not matter whether the number of neutrons beyond the $N = 126$ magic number is 4, 6 or 8. On the other hand, because of the influence of the 'α+ ^{208}Pb' cluster, ^{212}Po has a peculiar behaviour and its states should not be used to better characterize the two-body effective interactions at work in this mass region. A rather large amount of experimental data is now available in the major shell quadrant to the "north-east" of ^{208}Pb. They would deserve to be used in order to improve the SM predictions in the mass region between the doubly-magic ^{208}Pb core and the well-deformed actinides.

Acknowledgments

The Euroball project was a collaboration between France, the United Kingdom, Germany, Italy, Denmark and Sweden. We are very indebted to our colleagues involved in the EB-02/17 experiment devoted to the fission fragments, in which the present data on ^{214}Po were recorded. We thank the crews of the Vivitron, as well as M.-A. Saettle for preparing the Pb target, P. Bednarczyk, J. Devin, J.-M. Gallone, P. Médina and D. Vintache for their help during the experiment.

[1] ENSDF data base, http://www.nndc.bnl.gov/ensdf/.
[2] J. Kurpeta *et al.*, Eur. Phys. J. **A 7**, 49 (2000).
[3] H. De Witte *et al.*, Phys. Rev. **C69**, 044305 (2004).
[4] M.-G. Porquet, Int. J. Mod. Phys. **E13**, 29 (2004).
[5] A. Astier, P. Petkov, M.-G. Porquet, D.S. Delion, and P. Schuck, Phys. Rev. Lett. **104**, 042701 (2010).
[6] A. Astier, P. Petkov, M.-G. Porquet, D.S. Delion, and P. Schuck, Eur. Phys. J. **A 46**, 165 (2010).
[7] J. Simpson, Z. Phys. A**358**, 139 (1997).
[8] J. Eberth *et al.*, Nucl. Instr. Meth. A **369**, 135 (1996).
[9] G. Duchêne *et al.*, Nucl. Instr. Meth. A **432**, 90 (1999).
[10] D.C. Radford, Nucl. Instr. Meth. Phys. Res. A **361**, 297 and 306 (1995).
[11] A. Astier *et al.*, Eur. Phys. J. **A 30**, 541 (2006) and references therein.
[12] H.W. Taylor and B. Singh, Phys. Rev. **C40**, 449 (1989).
[13] Ts. Venkova *et al.*, Eur. Phys. J. **A 15**, 429 (2002).
[14] M.-G. Porquet *et al.*, Eur. Phys. J. **A 18**, 25 (2003).
[15] T. Kibédi *et al.*, Nucl. Instrum. Methods **A589**, 202 (2008), http://www.rsphysse.anu.edu.au/nuclear/bricc/.
[16] T. Yamazaki, Nucl. Data **A3**, 1 (1967).
[17] I. Talmi, *Simple Models of Complex Nuclei*, (Harwood Academic Publishers, 1993).